

Thermal Frequency Drift of Resonant Microsensor

F. Shen*, P. Lu*, S.J. O'Shea**, K. H. Lee*, S. C. Pradhan*, T. Y. Ng*

*Institute of High Performance Computing, 89C Science Park Drive,
#02-11/12 The Rutherford, Singapore 118261, shenf@ihpc.nus.edu.sg

**Institute of Materials Research & Engineering, 3 Research Link,
Singapore 117602

ABSTRACT

Thermal effects on the resonant frequency drift of a microsensor (a silicon cantilever beam with a gold coating) are studied. Two cases are investigated using analytical methods: uniform temperature distribution and linear temperature distribution along the length of the sensor. It is found that the thermal frequency drift is dominated by the temperature-dependent material properties. Thermal frequency drift also depends on the ratio of the thickness of the gold coating and the thickness of the silicon cantilever. The results show that the relationship between thermal frequency drift and the ratio of gold-to-silicon thickness is nearly linear.

Keywords: microsensor, silicon cantilever, resonant frequency, frequency drift, temperature dependence.

1 INTRODUCTION

Resonant microsensors can be used to detect very small sample masses. A change in the mass adsorbed on the sensor results in a change in the resonant frequency, which must be measured with high accuracy. It is therefore very important for the sensors to have high sensitivity and stability. Many factors will affect the resonant frequency response of the sensors and one of the main concerns is the temperature sensitivity [1]. Changes in the local environment or excitation and detection power can cause temperature changes of the sensors. Therefore, the resonant frequency of the sensors will drift due to thermal expansion and temperature-dependent properties of the materials [2,3]. It is found that for a single-crystal silicon beam, the thermal frequency drift $\Delta\omega/(\omega\Delta T)$ is in the range of $-27 \times 10^{-6}/K$ to $-56 \times 10^{-6}/K$ [3].

Typically the microsensors must be covered with some form of coating. Generally, more frequency drift will occur if the coating material has negative temperature coefficient of Young's modulus. Coating will also introduce thermal residual stress and cause bending of the resonant structure due to thermal mismatch. Proper selection of coating material can achieve smaller thermal frequency drift [4].

In this paper, we study the thermal drift of a micro-cantilever sensor with a gold coating. Apart from the uniform temperature case, which is usually caused by the change of environment temperature, we also study the linear temperature distribution case, which generally arises during excitation or detection. The effect on thermal drift of

the surface area covered by the coating is also studied. Since the coating layer in this study is very thin compared with the base silicon cantilever, bending effects due to thermal mismatch have not been included.

2 FREQUENCY DRIFT FOR UNIFORM TEMPERATURE DISTRIBUTION

For a cantilever, the resonant frequency can be expressed as follows:

$$\omega = \frac{\lambda^2}{l^2} \sqrt{\frac{E_s I_s + E_g I_g}{\rho_s A_s + \rho_g A_g}} \quad (1)$$

where E is Young's modulus, ρ the density, I the moment of inertia, A the cross sectional area of the cantilever, l the length of the cantilever and λ is a constant which depends on the constraint condition of the sensor. The subscripts s and g represent the silicon cantilever and gold coating, respectively.

The above expression can also be written as:

$$\omega = \frac{\lambda^2}{l^{3/2}} \sqrt{\frac{E_s I_s + E_g I_g}{m_s + m_g}} \quad (2)$$

where m_s and m_g are the masses of the silicon cantilever and gold coating, respectively. These mass terms are independent of the temperature.

For a composite beam, the moments of inertia are given by

$$I_s = \frac{1}{12} w t_s^3 + w t_s \left(h - \frac{1}{2} t_s \right)^2 \quad (3a)$$

$$I_g = \frac{1}{12} w t_g^3 + w t_g \left(t_s + \frac{1}{2} t_g - h \right)^2 \quad (3b)$$

where w is the width, t the thickness, and h is the distance between the neutral axis of the beam and the bottom surface, as shown in Figure 1, which can be expressed as:

$$h = \frac{E_s t_s^2 + E_g (t_g^2 + 2 t_s t_g)}{2 E_s t_s + 2 E_g t_g} \quad (4)$$

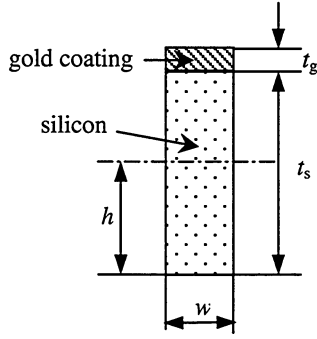


Figure 1: Cross section of the cantilever

Usually the coating layer is very thin and the Young's modulus of gold is about 1/3 of the Young's modulus of silicon. Hence, to simplify calculation, the value of h is determined as

$$h = \frac{1}{2}t_s \quad (5)$$

Differentiating equation (2) with respect to the temperature T and considering equations (3a), (3b) and (5), the frequency drift in terms of the ratio of thickness t_g/t_s can be obtained as,

$$\frac{1}{\omega} \cdot \frac{d\omega}{dT} = -\bar{\alpha} + \frac{1}{\frac{2}{3}E_s + 2E_g \left[\frac{1}{3} \cdot \left(\frac{t_g}{t_s} \right)^3 + \frac{t_g}{t_s} \left(1 + \frac{t_g}{t_s} \right)^2 \right]} \left\{ \frac{1}{3} \cdot \frac{dE_s}{dT} \right. \\ \left. + \left[\frac{1}{3} \cdot \left(\frac{t_g}{t_s} \right)^3 + \frac{t_g}{t_s} \left(1 + \frac{t_g}{t_s} \right)^2 \right] \cdot \frac{dE_g}{dT} + E_s \alpha_s + E_g \frac{t_g}{t_s} \left(1 + \frac{t_g}{t_s} \right) \right. \\ \left. \cdot \left[\left(1 + \frac{t_g}{t_s} \right) \alpha_g + 2 \left(\alpha_s + \frac{t_g}{t_s} \alpha_g \right) \right] \right\} \quad (6)$$

where, α_s and α_g are the thermal expansion coefficients of the silicon and gold, and

$$\bar{\alpha} = \frac{E_s A_s \alpha_s + E_g A_g \alpha_g}{E_s A_s + E_g A_g} \quad (7)$$

is the equivalent thermal expansion coefficient of the composite cantilever.

From the above expression, we can clearly see that the thermal frequency drift is linearly dependent on the temperature coefficients of the Young's moduli of the silicon beam and gold coating. The frequency drift also depends on the thickness ratio of the coating layer and the silicon beam. In addition, it can be observed that the frequency drift is independent of the cantilever length.

The relationship between the resonant frequency drift and the gold-to-silicon thickness ratio is shown in Figure 2. The material parameters used for the calculation are listed in

Table 1 [3,5]. Figure 2 shows that for thin coatings the thermal frequency drift increases almost linearly with increasing thickness of the gold coating. Nevertheless, the absolute value of the drift is dominated by the temperature dependent Young's modulus of the silicon, which at $t_g/t_s=0$ produces a drift of $(0.5/E_s)dE_s/dT = -27.2$ ppm/K.

Table 1: Material and geometry parameters

	E (GPa)	dE/dT(MPa/K)	α (m/m·K)
Silicon	202	-11	3×10^{-6}
Gold	78	-24	14.2×10^{-6}

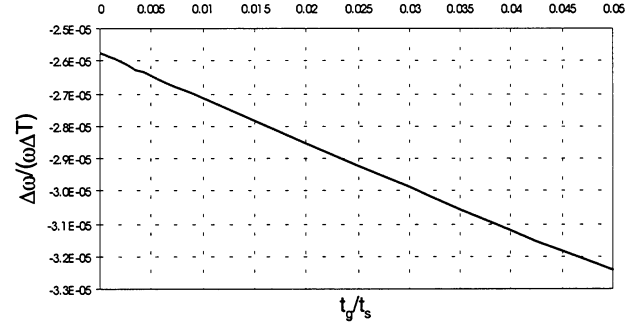


Figure 2: Relationship between thermal frequency drift and the ratio of thickness

3 FREQUENCY DRIFT FOR LINEAR TEMPERATURE DISTRIBUTION

In this case, it is assumed that the distribution of temperature is linear along the length of the cantilever. Due to the distributed temperature, the size of the cantilever as well as the material properties are functions of the variable x , which is the coordinate along the cantilever length. The governing partial differential equation for free vibration of the cantilever with gold coating can be expressed as:

$$\frac{\partial^2}{\partial x^2} \left\{ [E_s(x)I_s(x) + E_g(x)I_g(x)] \frac{\partial^2 v}{\partial x^2} \right\} + \\ [\rho_s(x)A_s(x) + \rho_g(x)A_g(x)] \frac{\partial^2 v}{\partial t^2} = 0 \quad (8)$$

where v is the transverse displacement of the cantilever.

Let $v(x, t) = V(x) \cdot e^{i\omega t}$, which gives,

$$\frac{d^2}{dx^2} \left\{ [E_s(x)I_s(x) + E_g(x)I_g(x)] \frac{d^2 V}{dx^2} \right\} - \\ [\rho_s(x)A_s(x) + \rho_g(x)A_g(x)] \omega^2 \cdot V = 0 \quad (9)$$

Equation (9) is a differential equation with non-constant coefficients. In general, the exact closed-form solutions are

not available. In this study, the coefficients are expressed in polynomial variation form, from which the fundamental solutions based on a power series can be obtained [6]. Let,

$$\xi = \frac{x}{l} \quad (10a)$$

$$\bar{V}(\xi) = \frac{V(x)}{l} \quad (10b)$$

$$G(\xi) = \frac{E_s(x)I_s(x) + E_g(x)I_g(x)}{E_s I_s + E_g I_g} = \sum_{i=0}^p g_i \xi^i \quad (10c)$$

$$Q(\xi) = \frac{\rho_s(x)A_s(x) + \rho_g(x)A_g(x)}{E_s I_s + E_g I_g} \omega^2 \cdot l^4 = \sum_{i=0}^q q_i \xi^i \quad (10d)$$

where E_s , E_g and I_s , I_g are the corresponding parameters at the reference temperature. The differential equation (9) can then be rewritten as:

$$\frac{d^2}{d\xi^2} \left[G(\xi) \cdot \frac{d^2 \bar{V}}{d\xi^2} \right] - Q(\xi) \cdot \bar{V} = 0 \quad (11)$$

The general solution of Eq. (11) takes the following form:

$$\bar{V}(\xi) = c_1 \bar{V}_1(\xi) + c_2 \bar{V}_2(\xi) + c_3 \bar{V}_3(\xi) + c_4 \bar{V}_4(\xi) \quad (12)$$

where c_1 , c_2 , c_3 and c_4 are constants and their values depend on the boundary conditions.

Assume that the four normalized fundamental solutions have the following forms:

$$\bar{V}_n(\xi) = \sum_{i=0}^{\infty} b_{n,i} \cdot \xi^i \quad n=1,2,3,4 \quad (13)$$

The above four fundamental solutions are linearly independent and can be chosen to satisfy the normalization conditions at the origin of coordinates [6] and the following coefficients can be determined:

$$\left. \begin{aligned} b_{1,0} &= 1, b_{1,1} = b_{1,2} = b_{1,3} = 0 \\ b_{2,1} &= 1, b_{2,0} = b_{2,2} = b_{2,3} = 0 \\ b_{3,2} &= \frac{1}{2}, b_{3,0} = b_{3,1} = b_{3,3} = 0 \\ b_{4,3} &= \frac{1}{6}, b_{4,0} = b_{4,1} = b_{4,2} = 0 \end{aligned} \right\} \quad (14)$$

Substituting Eq. (13) into the governing differential equation (11) and equating the coefficients with the same powers of ξ , the coefficients $b_{n,i}$ can be obtained as

$$b_{n,i+4} = \frac{1}{(i+1)(i+2)(i+3)(i+4)g_0}$$

$$\left[\sum_{j=0}^i b_{n,i-j} \cdot q_j - \sum_{j=1}^{i+2} (i+1)(i+2)(i-j+3)(i-j+4) \cdot b_{n,i-j+4} \cdot g_j \right] \quad n=1,2,3,4 \text{ and } i \geq 0 \quad (15)$$

By considering the boundary conditions and eliminating c_1 , c_2 , c_3 and c_4 , we obtain the following equation:

$$\sum_{i=2}^{\infty} \sum_{j=2}^{\infty} \sum_{k=0}^p i \cdot j \cdot (i-1) \cdot (j-1) \cdot (j+k-2) \cdot (b_{3,i} \cdot b_{4,j} - b_{4,i} \cdot b_{3,j}) \cdot g_k = 0 \quad (16)$$

By satisfying the above equation, the resonant frequency of the cantilever for a linear temperature distribution can be obtained.

Compared with the uniform temperature distribution case, the frequency drift for a linear temperature distribution depends additionally on the temperature difference between ambient temperature (T_r) and the temperature of the two ends of the cantilever (T_0 at the fixed end, T_1 at the free end). The temperature difference between the two ends is defined as ΔT ($T_0 - T_1$) and the temperature change at the free end is defined as ΔT_1 ($T_1 - T_r$).

Figure 3 shows how at fixed t_g/t_s , the frequency drift varies with temperature difference along the cantilever (ΔT) for various values of ΔT_1 . It is seen that at a fixed value of t_g/t_s , the frequency drift increases linearly with increasing ΔT . It is also noted that at fixed ΔT the frequency drift increases linearly with increasing ΔT_1 .

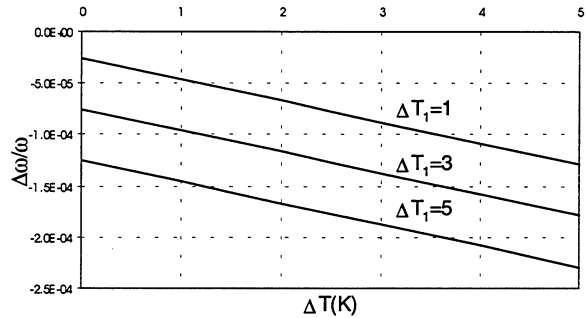


Figure 3: The effect of temperature increment ΔT_1 and temperature difference ΔT on frequency drift ($t_g/t_s=0.01$)

Figure 4 shows the relationship between frequency drift and the thickness ratio t_g/t_s for various values of ΔT and fixed temperature increment ΔT_1 . As in the uniform temperature case, the frequency drift varies almost linearly with t_g/t_s and increases as the thickness of the gold increases. The frequency drift increases as the temperature difference along the cantilever (ΔT) increases but most of this increased drift arises from an increase in the absolute temperature of the sensor structure. This can be seen by defining the free end temperature T_1 as the ambient temperature, from which it is found that there is negligible difference in the normalised temperature shift $\Delta\omega/(\omega\Delta T)$ for different ΔT .

Similarly, we can compare the normalised frequency drift $\Delta\omega/(\omega\Delta T)$ between the linear and uniform temperature cases by taking $\Delta T_1=0$ and $\Delta T=1$, as shown in Figure 5. In the linear case, the frequency drift is about 20% smaller for small t_g/t_s (<0.01). This reflects the fact that the average temperature rise of the sensor is smaller in the linear case.

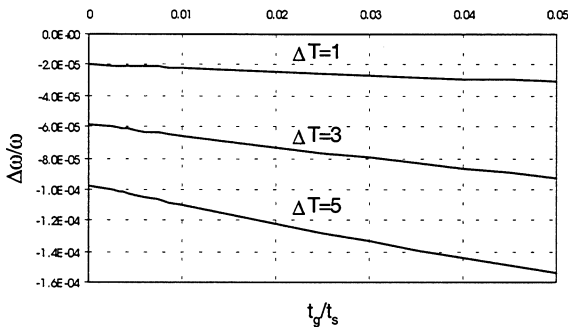


Figure 4: The effect of temperature difference ΔT and ratio of thickness on frequency drift ($\Delta T_1=0$)

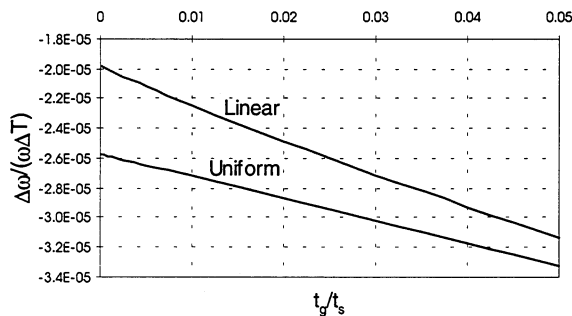


Figure 5: Comparison of frequency drift for uniform and linear temperature distributions

4 EFFECT OF THE COATING AREA

In the above analyses, we assume that the gold coating covers the entire surface of the silicon beam. However, in practical applications it may not be necessary to coat the entire cantilever surface.

In order to investigate thermal effects arising from the surface area covered by the coating, we assume that the temperature is uniform so that an analytical solution can be applied. We can then separate the cantilever into two regions of constant cross section as shown in Figure 6, with one region representing an area coated by gold (length l_g) and one region bare silicon (length $l-l_g$). By satisfying the boundary conditions and the continuity conditions at the connecting section, the temperature dependence of the resonant frequency can be obtained.

Figure 7 shows the thermal frequency drift as a function of the coating area, which is proportional to l_g/l . It is seen that the frequency drift increases approximately linearly between the uncoated case and the fully coated case. For thin films ($t_g/t_s=0.01$) it is seen that the temperature drift is dictated by the silicon cantilever.

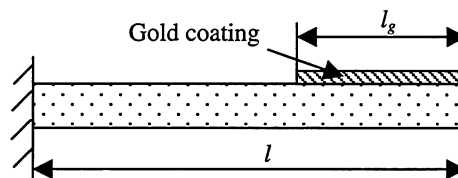


Figure 6: Partly coated cantilever

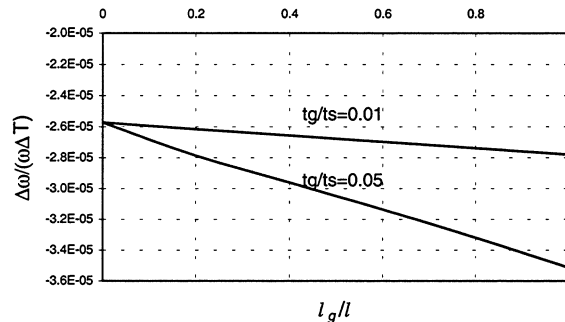


Figure 7: The effect of coating area on thermal drift

5 CONCLUSION

The thermal frequency drift of a silicon microsensor with gold coating has been studied. Two general temperature distributions have been discussed, namely uniform and linearly variable. It has been shown that the thermal frequency drift is dominated by the temperature-dependent Young's modulus of the cantilever materials. The gold coating will cause additional thermal drift because of the negative temperature coefficient of Young's modulus. In both the uniform and linear temperature distribution cases, the thermal drift varies approximately linearly with the silicon-to-gold thickness ratio. The thermal drift is about 20% lower for linear case at small t_g/t_s (<0.01). The methods outlined in this paper can be used to assist in the design of microsensors for which low temperature sensitivity is desirable.

REFERENCES

- [1] G. Stemme, *J. Micromech. Microeng.* 1, 113-125, 1991.
- [2] R. A. Buser and N. F. De Rooij, *Sensors and Actuators*, 17, 145-154, 1989.
- [3] M. J. Tudor, M. V. Andres, K. W. H. Foulds and J. M. Naden, *IEE Proceedings*, 135(5), 364-368, 1988.
- [4] M. B. Othman and A. Brunnschweiler, *Electronics Letters*, 23(14), 728-730, 1987.
- [5] J. E. Sader, I. Larson, P. Mulvaney and L. R. White, *Rev. Sci. Instrum.* 66(7), 3789-3798, 1995.
- [6] S. Y. Lee, and Y. H. Kuo, *Journal of Applied Mechanics*, 59, S205-S212, 1992.